

Approaches to relativistic positioning around Earth and error estimations

Neus Puchades^a, Diego Sáez^{a,b}

^a*Departamento de Astronomía y Astrofísica, Universidad de Valencia, 46100-Burjassot, Valencia, Spain.*

^b*Observatorio Astronómico, Universidad de Valencia, 46980 Paterna, Valencia, Spain*

Abstract

In the context of relativistic positioning, the coordinates of a given user may be calculated by using suitable information broadcast by a 4-tuple of satellites. Our 4-tuples belong to the Galileo constellation. Recently, we estimated the positioning errors due to uncertainties in the satellite world lines (U-errors). A distribution of U-errors was obtained, at various times, in a set of points covering a large region surrounding Earth. Here, the positioning errors associated to the simplifying assumption that photons move in Minkowski space-time (S-errors) are estimated and compared with the U-errors. Both errors have been calculated for the same points and times to make comparisons possible. For a certain realistic modeling of the world line uncertainties, the estimated S-errors have proved to be smaller than the U-errors, which shows that the approach based on the assumption that the Earth's gravitational field produces negligible effects on photons may be used in a large region surrounding Earth. The applicability of this approach –which simplifies numerical calculations– to positioning problems, and the usefulness of our S-error maps, are pointed out. A better approach, based on the assumption that photons move in the Schwarzschild space-time governed by an idealized Earth, is also analyzed. More accurate descriptions of photon propagation involving non symmetric space-time structures are not necessary for ordinary positioning and spacecraft navigation around Earth.

Keywords: General relativity; Relativistic positioning systems; Global navigation satellite systems; Methods: numerical

Email address: diego.saez@uv.es (Diego Sáez)

1. Introduction

This paper focuses on the estimation of positioning errors in some relativistic positioning systems (RPS). Realizations of RPS must be based on general relativity (GR); more specifically, the following theoretical scheme is to be implemented:

(i) Space-time is governed by an energy distribution including Earth, Sun and other sources. It is described by a metric, which must be written in terms of certain coordinates, y^α , being appropriate to deal with positioning.

(ii) In the absence of non gravitational forces, satellites and photons move in the aforementioned space-time as test particles; namely, following geodesics. In particular, satellites follow time-like geodesics which may be parametrized by the proper times.

(iii) Once the metric and the world lines of satellites and photons are known, any user may calculate its y^α coordinates by using the proper times broadcast by four satellites, the so-called emission coordinates τ^A .

(iv) These emission coordinates and the satellite world lines –parametrized by the proper times– set the satellite coordinates at emission, which are also the initial photon coordinates; namely, the coordinates at the starting point of the photons broadcasting information.

(v) Among the photon geodesics it is possible to find four intersecting ones (one per satellite), and the coordinates y^α of the resulting intersection event define the user position.

Any approach to RPS based on these general ideas requires additional assumptions and approximations.

In our opinion, the estimation of positioning errors is more systematic in the RPS context. Instead of applying a correction for each effect leading to errors, let us systematically proceed taking into account the following points:

(1) We define *nominal satellite world lines*, which are appropriate time-like geodesics of the RPS space-time. These geodesics would be the true satellite world lines in the absence of perturbations

(2) In a given RPS, there are non gravitational perturbations such as solar winds, radiation pressure, and so on, as well as gravitational perturbations due to the energy sources which have not been taken into account to fix the space-time structure. All these perturbations would produce growing deviations with respect to the nominal world lines

(3) These deviations will not be estimated but controlled; namely, the satellite world lines will be corrected as soon as the amplitude of their deviations reaches a certain limit value

(4) The amplitude evolution and the statistical character of the deviations will be determined from the analysis of many data, which may be obtained by measuring deviations over an extended period (many satellite periods)

(5) Once nominal world lines and statistical realizations of the deviations are available, the nominal world lines will be used to calculate the user position, and the deviations to estimate errors. These errors will be hereafter called U-errors since they are due to uncertainties in the satellite world lines

(6) The best RPS would be obtained taking into account all the sources contributing to the gravitational field. In such a case, only the non gravitational forces would produce deviations with respect to the nominal world lines and, consequently, less corrections of the satellite motions would be necessary to maintain the deviations smaller than the chosen limit amplitude.

(7) There are other positioning errors associated to the description of photon propagation (from the satellites to the user). These errors arise when some sources of the gravitational field are neglected and, consequently, the metric and the photon null geodesics are not fully accurate.

Two approaches to relativistic positioning are considered in this paper, in both cases we look for the positioning coordinates and their errors. These RPS are designed by assuming that the space-time has the Schwarzschild metric, which corresponds to an ideal isolated static spherically symmetric Earth. Schwarzschild space-time is asymptotically Minkowskian and, consequently, once the approach based on Schwarzschild metric is assumed, one can say that, from a theoretical (physical) point of view, there are inertial (quasi inertial) systems of reference. The origin of these references is located in the Earth's center and the spatial axes are arbitrary. The simplest of these two approaches, hereafter called the 0-order RPS, is based on the following assumptions: (a) satellite world lines are time-like geodesics of the Schwarzschild space-time (hereafter S-ST), and (b) photons follow null geodesics in the Minkowski space-time (M-ST) asymptotic to the Schwarzschild space-time. In a more accurate approach, hereafter called the 1-order RPS, both satellites and photons move in S-ST. Here, the accuracy of the 0-order RPS is quantitatively estimated, for the first time, in an extended region surrounding Earth. This estimation is based on the calculation of the S-errors, which are the differences between the positioning coordinates obtained in the 0 and 1-order RPS.

In [Puchades and Sáez \(2014\)](#), the U-errors were estimated inside a spherical region, with radius $R = 10^5 \text{ km}$, centered at point E. The spherical inertial coordinates of E were assumed to be $r_E = R_\oplus$, $\theta_E = 60^\circ$, and $\phi_E = 30^\circ$, where R_\oplus is the Earth’s radius. Hence, point E is on the Earth’s surface. It is an arbitrary point and results do not depend on its choice. In this paper, other positioning errors (S-errors) are estimated inside the same sphere to facilitate comparisons with the U-errors. This great region around Earth is hereafter referred to as the E-sphere.

We only consider the Galileo constellation, whose satellites are being placed in orbit by the European Space Agency. This GNSS (global navigation satellite system) has 27 satellites, which are uniformly distributed on three equally spaced orbital planes. We have numbered the satellites in such a way that numbers 1 to 9, 10 to 18, and 19 to 27 correspond to consecutive orbital planes. Inside any of these planes, satellites n and $n + 1$ occupy successive positions. The inclination of these planes is $\alpha_{in} = 56$ degrees and the altitude of the circular orbits is $h = 23222 \text{ km}$; thus, the orbital period is about 14 h . See [Pascual-Sánchez \(2007\)](#) for details. Our nominal world lines are chosen to be Schwarzschild time-like geodesics with these circular orbits.

Let us make some comments about notation and units which will be taken into account in the whole paper. Index A labels the four satellites necessary for space-time positioning; any other Latin index runs from 1 to 3, and Greek indexes from 1 to 4. Quantities G , M_\oplus , t , and τ stand for the gravitation constant, the Earth’s mass, the coordinate time, and the proper time, respectively. In our numerical codes, units are chosen in such a way that the speed of light is $c = 1$; the kilometer is the unit of distance, and times are given in units of $10^{-5}/3 \text{ s}$ (hereafter *code units*). In all the equations we set $c = 1$ and, finally, results (code outputs) are presented in appropriate arbitrary units of distance and time.

The paper is structured as follows: the 0-order RPS is briefly described in Sect. 2. The 1-order RPS, is studied in Sect. 3. The S-errors are analyzed in Sect. 4, where they are compared with previously estimated U-errors ([Puchades and Sáez, 2014](#)). Main conclusions are briefly summarized in Sect. 5, where a general discussion is also presented.

2. Emission and inertial coordinates in the 0-order RPS

In the 0-order RPS, positioning coordinates are inertial coordinates in the M-ST asymptotic to S-ST and, consequently, they will be called *inertial*

asymptotic coordinates or inertial coordinates x^α , as done in previous papers (Puchades and Sáez, 2012; Sáez and Puchades, 2013; Puchades and Sáez, 2014).

The inertial coordinates (user position) may be found by using the satellite world lines and the emission proper times, excepting some cases in which the emission coordinates are compatible with two user positions (bifurcation); in these cases, a criterion –based on additional data– is necessary to choose the true position (Schmidt, 1972; Abel and Chaffee, 1991; Chaffee and Abel, 1994; Grafarend and Shan, 1996; Coll et al., 2011, 2012; Puchades and Sáez, 2012). Bifurcation does not play a role in this paper.

In any asymptotic inertial reference, calculation of the user position requires knowledge of the satellite world lines. If the equations of these lines are expressed in terms of the proper time parameter, the coordinates of their points are functions of the form $x_A^\alpha = x_A^\alpha(\tau^A)$. Whichever the satellite world lines may be, if photons move along null geodesics in M-ST (from emission to user reception), the emission coordinates, τ^A , and the inertial coordinates, x^α , are related as follows:

$$\eta_{\alpha\beta}[x^\alpha - x_A^\alpha(\tau^A)][x^\beta - x_A^\beta(\tau^A)] = 0 , \quad (1)$$

where $\eta_{\alpha\beta}$ is the M-ST metric tensor, whose non vanishing components are $\eta_{11} = \eta_{22} = \eta_{33} = 1$ and $\eta_{44} = -1$.

Given a point Q of the M-ST with coordinates x^α , Eqs. (1) may be numerically solved to get the emission proper times τ^A , which would be the emission coordinates received by an user at Q . A multiple precision numerical code has been designed to perform this calculation –leading to τ^A – for an arbitrary Q . It is hereafter referred to as the XT-code. This code uses both the satellite world line equations and the numerical Newton-Raphson method (Press et al., 1999).

Coll et al. (2010) derived an analytical solution of Eqs. (1), which gives x^α in terms of τ^A for photons moving in M-ST. A numerical code based on this solution –hereafter referred to as the TX-code– has been designed and tested (Puchades and Sáez, 2011, 2012; Sáez and Puchades, 2013, 2014; Puchades and Sáez, 2014). The analytical solution holds for arbitrary satellite world lines; hence, these lines may be identified with the nominal world lines of four Galileo satellites (see Sect. 1), whose equations may be written in terms of the asymptotic inertial coordinates and the proper time. These equations are given in Sect. 3.

In practice, perturbations deviate any satellite from its nominal world line and, consequently, there are U-errors, which were estimated –in [Sáez and Puchades \(2013\)](#); [Puchades and Sáez \(2014\)](#)– under the assumption that the satellite world lines are systematically corrected to always have space (time) deviations –with respect to the nominal world lines– which are smaller than $10^{-2} km$ (10^{-2} code units of time) [see [Puchades and Sáez \(2014\)](#) for more details].

3. Relativistic positioning in S-ST: the 1-order RPS

Various concepts and techniques being useful to develop the 1-order RPS have been found in previous papers, among them, we may point out the definition and uses of the world function ([Synge, 1931](#); [Bahder, 2001](#); [Bini et al., 2008](#); [San Miguel, 2007](#)) and the time transfer function, the form of this last function in the S-ST ([Teyssandier and Le Poncin-Lafitte, 2008](#)), and a method to find the user position coordinates by using the time transfer function ([Čadež and Kostić, 2005](#); [Čadež et al., 2010](#); [Delva et al., 2011](#)). Here, this last method is modified by using the analytical formula derived by [Coll et al. \(2010\)](#) –instead of numerical iterations– to work with photons moving in M-ST

The Earth’s center is at rest in the asymptotic M-ST; hence, the S-ST may be considered as a perturbation of the asymptotic M-ST with a static metric $g_{\alpha\beta} = \eta_{\alpha\beta} + s_{\alpha\beta}$, where $\eta_{\alpha\beta}$ is the Minkowski metric, and $s_{\alpha\beta}$ are perturbation terms depending on GM_{\oplus}/R , where R is the Schwarzschild radial coordinate.

The S-errors are due to the lensing deviations produced by the 1-order RPS gravitational field, and these deviations are integrated effects on the full paths traveled by the photons (from satellites to users). Since the length of these paths has an order of magnitude whose values are $\sim 10^4 km$ for users on Earth and $\sim 10^5 km$ for users on the surface of the E-sphere (see [Sect. 1](#)) and, moreover, all the admissible nominal world lines must be very close among them (with deviations smaller than $10 m$), it is evident that the photon paths, the lensing integrated effect, and the S-errors will be almost identical for any admissible choice of the nominal lines. On account of this fact, the nominal world lines of the Galileo satellites may be assumed to be time-like geodesics of the S-ST with circular orbits. This simple choice is good enough to compute S-errors and, moreover, it allows comparisons with the U-errors calculated in [Puchades and Sáez \(2014\)](#), where the same nominal world lines were used.

In the unperturbed M-ST, the spatial location of a Galileo satellite A , which moves along a circumference, requires three angles. Two of them, Θ and ψ , characterize one of the three orbital planes. These angles are constant. The third angle, α_A , localizes the satellite on its trajectory. It depends on time. All this was taken into account in [Puchades and Sáez \(2012, 2014\)](#) to find the world line equations of the satellite A to first order in the small dimensionless parameter GM_\oplus/R , whose maximum value is $GM_\oplus/R_\oplus \simeq 6.94 \times 10^{-10}$. These equations are as follows:

$$\begin{aligned} x_A^1 &= R [\cos \alpha_A(\tau) \cos \psi + \sin \alpha_A(\tau) \sin \psi \cos \Theta] \\ x_A^2 &= -R [\cos \alpha_A(\tau) \sin \psi - \sin \alpha_A(\tau) \cos \psi \cos \Theta] \\ x_A^3 &= -R \sin \alpha_A(\tau) \sin \Theta \\ x_A^4 &= \gamma \tau, \end{aligned} \tag{2}$$

where the factor γ and the angle α_A are given by the relations ([Ashby, 2003](#); [Pascual-Sánchez, 2007](#))

$$\gamma = \frac{dt}{d\tau} = \left(1 - \frac{3GM_\oplus}{R}\right)^{-1/2} \tag{3}$$

and

$$\alpha_A(\tau) = \alpha_{A0} - \Omega \gamma \tau, \tag{4}$$

respectively. The last equation involves the satellite angular velocity $\Omega = (GM_\oplus/R^3)^{1/2}$, and the angle α_{A0} fixing the position of satellite A at $\tau = x^4 = 0$ (GNSS initial operation time). The chosen nominal world lines satisfy Eqs. (2)–(4).

Let us now assume that a certain set of four emission coordinates, τ^A , has been received. By using these coordinates, the user position may be found in both the 0 and 1-order RPS. In the first case, photons move in the asymptotic M-ST, whereas for the 1-order RPS, photons move in the proper S-ST and calculations are performed up to first order in GM_\oplus/R . Thus, two different positions are obtained, which allow us to estimate the positioning S-error. In both cases, Eqs. (2)–(4) allow us to compute the position of any Galileo satellite (coordinates x_A^μ) for any proper time τ . Hence, from the four emission coordinates τ^A , we may calculate the positions of the four satellites, at emission times, in S-ST. These emission events define the initial common points of the two photon world lines (in M-ST and S-ST); for this reason, these events are denoted P_{IA} , and $x_{IA}^\mu(\tau^A)$ are their asymptotic inertial coordinates in S-ST.

We first assume that photons move in S-ST. Those emitted from the satellite A initiate their motion at the point P_{IA} whose coordinates $x_{IA}^\mu(\tau^A)$ have been calculated from τ^A . The user position is then the intersection of four null geodesics that pass through points P_{IA} and have appropriate propagation directions at these points. The coordinates of the intersection point P_{S0} (user space-time position in S-ST) are denoted x_{S0}^μ . Since the propagation directions are unknown, a suitable method is necessary to find the intersection point; namely, to localize the user. A first version of the method used here, which does not use the exact solution of [Coll et al. \(2010\)](#), was implemented by [Delva et al. \(2011\)](#). Let us now describe our version of this method, which uses this exact solution. Both versions are based on the fact that, for the geodesic passing through points P_{IA} and P_S (coordinates x_S^μ), there is a relation between $x_S^4 - x_{IA}^4 \equiv t_S - t_{IA}$ and the coordinates $x_{IA}^i \equiv \vec{R}_{IA}$ and $x_S^i \equiv \vec{R}_S$. This relation may be written in the form

$$t_S - t_{IA} = T_S(\vec{R}_{IA}, \vec{R}_S) , \quad (5)$$

where $t_S - t_{IA}$ is the time elapsed from emission to event P_S , and T_S is the so-called time transfer function corresponding to S-ST.

Let us now consider that the photons emitted from the points P_{IA} –with coordinates $x_{IA}^\mu(\tau^A)$ – follow null geodesics in the asymptotic M-ST. Four of these geodesics intersect at point P_{M0} (user space-time position in M-ST), whose coordinates x_{M0}^μ are to be compared with x_{S0}^μ . As in the S-ST, the time elapsed to go –along a null geodesic– from the emission event to a point Q_M with coordinates (x_M^i, t_M) may be written as follows:

$$t_M - t_{IA} = T_M(\vec{R}_{IA}, \vec{R}_M) , \quad (6)$$

where T_M is the time transfer function of the asymptotic M-ST. In this simple geometry, the null geodesics are straight lines and, consequently,

$$T_M(\vec{R}_{IA}, \vec{R}_M) = |\vec{R}_M - \vec{R}_{IA}| . \quad (7)$$

Quantities (\vec{R}_{M0}, t_{M0}) ; namely, the user asymptotic inertial coordinates x_{M0}^μ may be calculated, from the emission coordinates τ^A , by using the TX-code (see Sect. 2) This code calculates all the possible user positions corresponding to given τ^A coordinates. We can find either one or two positions (bifurcation). Hence, from the emission coordinates τ^A , we have described suitable methods to calculate: x_{IA}^i , t_{IA} , x_{M0}^i , and t_{M0} . In the bifurcation

case, there are two pairs (x_{M0}^i, t_{M0}) which may be separately considered. Once a pair has been fixed, the positioning solution in M-ST (0-order RPS) is corrected to get the corresponding solution in the 1-order RPS; namely, in S-ST. This correction may be estimated as follows: first of all, for any point Q_M of the null geodesic passing through the emission and reception events in M-ST, an associated point P_S of the corresponding null geodesic in S-ST is defined by the relation $x_S^\mu(P_S) = x_M^\mu + \Delta x_M^\mu$. Thus, Eq. (5) may be rewritten as follows:

$$t_M + \Delta t_M - t_{IA} = T_S(\vec{R}_{IA}, \vec{R}_M + \Delta \vec{R}_M) . \quad (8)$$

The right hand side of this equation may be expanded up to first order in $\Delta \vec{R}_M$ to get:

$$t_M + \Delta t_M - t_{IA} = T_S(\vec{R}_{IA}, \vec{R}_M) + \frac{\partial T_S(\vec{R}_{IA}, \vec{R}_S)}{\partial \vec{R}_S} \Big|_{\Delta \vec{R}_M=0} \cdot \Delta \vec{R}_M . \quad (9)$$

Since Δt_M is a first order quantity, all the terms in Eq. (9) must be developed up to this order; hence, function $T_S(\vec{R}_{IA}, \vec{R}_M)$ is to be expanded up to first order, but the gradient involved in Eq. (9) is only required at zero order, since it is multiplied by the first order quantity $\Delta \vec{R}_M$.

At zero order, S-ST is identical to M-ST and, consequently, taking into account Eq. (7) one finds $T_S(\vec{R}_{IA}, \vec{R}_M) = |\vec{R}_M - \vec{R}_{IA}| + O(1)$; namely, the zero order approximation of the Schwarzschild time transfer function is $T_S^{(0)}(\vec{R}_{IA}, \vec{R}_M) = |\vec{R}_M - \vec{R}_{IA}|$. Hence, at zero order, the gradient of Eq. (9) may be written in the form:

$$\frac{\partial T_S(\vec{R}_{IA}, \vec{R}_S)}{\partial \vec{R}_S} \Big|_{\Delta \vec{R}_M=0}^{(0)} = \frac{\vec{R}_M - \vec{R}_{IA}}{|\vec{R}_M - \vec{R}_{IA}|} . \quad (10)$$

It has been proved that T_S may be expanded as follows [see [Teyssandier and Le Poncin-Lafitte \(2008\)](#) and references cited therein]:

$$T_S = |\vec{R}_M - \vec{R}_{IA}| + T_S^{(1)} + O(2) , \quad (11)$$

with

$$T_S^{(1)} = 2GM_\oplus \ln \left[\frac{|\vec{r}_M| + |\vec{r}_{IA}| + |\vec{r}_M - \vec{r}_{IA}|}{|\vec{r}_M| + |\vec{r}_{IA}| - |\vec{r}_M - \vec{r}_{IA}|} \right] , \quad (12)$$

where $r = |\vec{r}| = |\vec{R}|(1 - GM_\oplus/|\vec{R}|)$ is the so-called radial isotropic coordinate [see [Misner et al. \(1973\)](#)].

From Eqs. (6), (9), and (10)–(12), one easily gets

$$\begin{aligned} \Delta t_M - \frac{\vec{R}_M - \vec{R}_{IA}}{|\vec{R}_M - \vec{R}_{IA}|} \cdot \Delta \vec{R}_M = \\ 2GM_\oplus \ln \left[\frac{|\vec{r}_M| + |\vec{r}_{IA}| + |\vec{r}_M - \vec{r}_{IA}|}{|\vec{r}_M| + |\vec{r}_{IA}| - |\vec{r}_M - \vec{r}_{IA}|} \right]. \end{aligned} \quad (13)$$

These equations must be particularized at point $\vec{R}_M = \vec{R}_{M0}$ and $t_M = t_{M0}$. After particularization, there are four equations to find the four unknowns $\Delta \vec{R}_{M0}$ and Δt_{M0} and, then, the positioning coordinates in S-ST are $\vec{R}_{S0} = \vec{R}_{M0} + \Delta \vec{R}_{M0}$ and $t_{S0} = t_{M0} + \Delta t_{M0}$. Each of the four Eqs. (13) corresponds to a particular satellite (index A). The determinant of the particularized system of four equations is

$$D = \begin{vmatrix} \frac{x_{I1}^1 - x_{M0}^1}{|\vec{R}_{M0} - \vec{R}_{I1}|} & \frac{x_{I1}^2 - x_{M0}^2}{|\vec{R}_{M0} - \vec{R}_{I1}|} & \frac{x_{I1}^3 - x_{M0}^3}{|\vec{R}_{M0} - \vec{R}_{I1}|} & 1 \\ \frac{x_{I2}^1 - x_{M0}^1}{|\vec{R}_{M0} - \vec{R}_{I2}|} & \frac{x_{I2}^2 - x_{M0}^2}{|\vec{R}_{M0} - \vec{R}_{I2}|} & \frac{x_{I2}^3 - x_{M0}^3}{|\vec{R}_{M0} - \vec{R}_{I2}|} & 1 \\ \frac{x_{I3}^1 - x_{M0}^1}{|\vec{R}_{M0} - \vec{R}_{I3}|} & \frac{x_{I3}^2 - x_{M0}^2}{|\vec{R}_{M0} - \vec{R}_{I3}|} & \frac{x_{I3}^3 - x_{M0}^3}{|\vec{R}_{M0} - \vec{R}_{I3}|} & 1 \\ \frac{x_{I4}^1 - x_{M0}^1}{|\vec{R}_{M0} - \vec{R}_{I4}|} & \frac{x_{I4}^2 - x_{M0}^2}{|\vec{R}_{M0} - \vec{R}_{I4}|} & \frac{x_{I4}^3 - x_{M0}^3}{|\vec{R}_{M0} - \vec{R}_{I4}|} & 1 \end{vmatrix}. \quad (14)$$

If this determinant vanishes for the emission coordinates τ^A , there is no solution to the corresponding system of equations, which means that positioning at the M-ST point P_{M0} [with coordinates (x_{M0}^i, t_{M0})] is not possible. Close to a point of this kind, the determinant must be small and, consequently, the deviations $\Delta \vec{R}_{M0}$ and Δt_{M0} are expected to be large. Let us now raise the following question: are there emission coordinates leading to a vanishing determinant?

Following [Puchades and Sáez \(2014\)](#), the value of $|D|$ is just $6V_T$, where V_T stands for the volume of the *tetrahedron formed by the tips of the four user-satellite unit vectors*, which have their common origin at point (\vec{R}_{M0}, t_{M0}) in M-ST. See also [Langley \(1999\)](#), where this volume was related with the so-called dilution of precision (U-errors). If the four unit vectors mentioned above correspond to generatrices of the same cone, their tips are on the same plane and, consequently, the volume V_T vanishes; hence, the answer to the

above question is positive. In other words, there are degenerate configurations leading to vanishing D , in which, the user would see the four satellites on the same circumference.

If a spacecraft carries devices to get the line of sight of any visible Galileo satellite at emission time, the volume $V_T = |D|/6$ may be estimated for any visible 4-tuple and, consequently, 4-tuples leading to excessively small $|D|$ values may be rejected. After improvements, this method for 4-tuple selection might help us to design a good autonomous spacecraft navigation system –up to distances around 10^5 km– based, e.g., on Galileo satellites.

The regions where the S-errors are expected to be too large must be located either close to points where D vanishes, or at points located very far from the satellites. At these last points, the four satellites are all in a small solid angle and the tetrahedron volume V_T is expected to be small. Our numerical estimates are in agreement with these expectations (see next sections). The same is also valid for the U-errors estimated in [Puchades and Sáez \(2014\)](#).

4. Numerical analysis

In practice, the user –whose position is unknown– receives four emission proper times τ^A , which may be used to get two sets of inertial coordinates (positions). One of them corresponds to null geodesics in M-ST and the other one to photon motions in S-ST. Nevertheless, in order to get a distribution of positioning S-errors, we may proceed as follows: Given four satellites of the Galileo constellation, and a user position (x_{M0}^i, t_{M0}) in M-ST, whose coordinates x_{M0}^i correspond to a point of the E-sphere (see Sect. 1), the XT-code (see Sect. 2) may be used to get the emission coordinates τ^A which would be received by the chosen M-ST user. From these emission coordinates and the satellite world lines in S-ST [Eqs. (2)–(4)], the initial photon positions (x_{IA}^i, t_{IA}) may be obtained and, then, the S-errors at the M-ST chosen point (x_{M0}^i, t_{M0}) may be calculated by solving Eqs. (13) for the unknowns Δx_{M0}^i and Δt_{M0} . Quantities $\Delta_R = \Delta |\vec{R}_{M0}|$ and $\Delta_t = \Delta t_{M0}$ are good estimators of the S-errors.

4.1. General considerations

For a comparison with previous calculations of U-errors, which is necessary to decide if the 0 and 1-order RPS may be applied to a given positioning problem, the determinant D and the estimators Δ_R and Δ_t must be calculated for appropriate satellite 4-tuples and users (space-time points). These

quantities have been found for a set of $t = \textit{constant}$ space-time hypersurfaces, in many points conveniently placed on four great spheres with different radii and concentric with Earth. These spheres are inside the E-sphere. The same points and spheres were already considered to calculate U-errors (see [Puchades and Sáez \(2014\)](#) for details).

We have considered many 4-tuples and hypersurfaces of constant time (hereafter given in hours), but the main properties of the S-errors may be pointed out by using only the 4-tuple 2, 5, 20, and 23, and the hypersurface $t = 19$, as done in the rest of this paper.

As done in ([Puchades and Sáez, 2014](#)), the spheres are pixelized by using the HEALPIX package, which was designed to build up temperature maps of the cosmic microwave background (CMB). Quantities Δ_R and Δ_t are calculated for users located at the centers of the HEALPIX pixels and, then, pixels are colored (color bar) to show the value taken by Δ_R or Δ_t in them. Colors outside the bar may be used to mark special pixels; in particular, pixels where the represented quantity is not defined or it satisfies some condition.

Finally, the mollweide projection is used to show, in unique figure, the whole pixelized colored sphere. The frontal hemisphere is represented in the central part of the figure, and the opposite hemisphere is projected on the lateral parts. The external edges of these parts represent the same back semi-meridian. HEALPIX-mollweide CMB maps may be seen, e.g., in [Bennett et al. \(2013\)](#).

Figs. 4 and 5 show HEALPIX-mollweide maps. The interpretation of these Figures only requires: the definition of the quantities represented in the maps, and the rules used to assign colors which are not in the bar (special pixels). This information is given in the figure captions. Interpretations are detailed in the text.

In [Górski et al. \(1999\)](#), the reader may find more details about the HEALPIX pixelization, which is a hierarchical equal area isolatitude pixelization of the sphere. The number of pixels is $12 \times N_{side}^2$, where the free parameter N_{side} takes on even natural values. All the HEALPIX pixels have not the same shape, they are more elongated in the polar zones. In our maps, the HEALPIX parameter N_{side} is chosen to have 3072 pixels and, then, the angular area subtended by each of these pixels is close to sixty four times the mean angular area of the full moon (~ 13.43 squared degrees). The angular separation between the directions associated to two neighboring equatorial pixels is $\Delta\alpha \simeq 0.1 \textit{ rad}$. We have verified that this pixelization is adequate for our purposes.

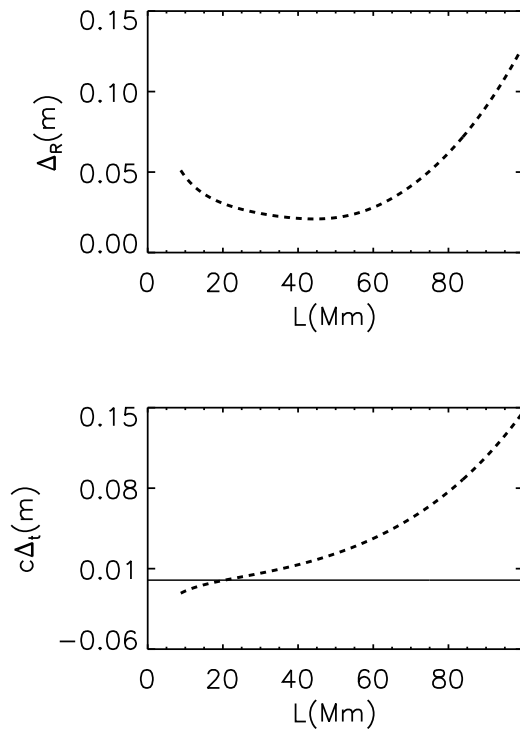


Figure 1: The values of Δ_R (top) and $c\Delta_t$ (bottom) [in meters] are represented in terms of the distance L to point E in megameters. This representation corresponds to a typical direction without any $D = 0$ point

For a given 4-tuple of satellites, positioning is only possible if the user may see the four satellites at the same time (visibility points). On account of this fact, we proceed as follows: (a) the users which do not see the four satellites (invisibility points) are identified, (b) the corresponding S-errors are not calculated and, (c) these users are properly marked in graphic representations.

4.2. S-errors along typical radial directions

Quantities Δ_R and Δ_t have been also calculated, along many HEALPIX directions, at points whose distances L to E range from $L = 0$ to $L = 10^5$ km. The values corresponding to three characteristic directions are now presented. Results are displayed in Figs. 1–3.

The first direction (Fig. 1) does not contain any $D = 0$ point and we see that, for large enough L values, the estimators Δ_R and $|\Delta_t|$ are continuous

increasing functions of L . From point E ($L = 0$) to the starting point of the curve of Fig. 1 ($L \simeq 8800 \text{ km}$), there is an invisibility segment since Earth –very close to the users in this segment– hides one or more satellites of the chosen 4-tuple. In Figs. 2 and 3, the length of the corresponding segment is 16700 and 16800 km , respectively.

The second direction (Fig. 2) contains only a $D = 0$ point at $L \simeq 73300 \text{ km}$. In the top and the middle-bottom panels of this Figure, the position of the $D = 0$ point is the center of the Δ_R peak and the Δ_t discontinuity, respectively. Around the $D = 0$ point, quantities Δ_R and $|\Delta_t|$ are very large. In the middle-top and bottom panels, only the values of these quantities smaller than 2 m have been represented; hence, in the region between the two dashed lines of these panels, Δ_R and $|\Delta_t|$ take on values greater than two meters. In this case, we easily see that values of two meters arise at distances (hereafter 2m-distances $\equiv \Delta L_{2m}$) of various thousands of kilometers from the $D = 0$ point. In these units, the inequality $3400 \leq \Delta L_{2m} \leq 6200$ is satisfied.

Finally, Fig. 3 corresponds to a third particular direction with two $D = 0$ points located at distances $L \simeq 27400 \text{ km}$ and $L \simeq 40000 \text{ km}$. This Figure has the same structure as Fig. 2. Two peaks and two discontinuities –giving the location of the two $D = 0$ points– are observed in the top and middle-bottom panels. As it follows from the middle-top and bottom panels of Fig. 3, quantities Δ_R and $|\Delta_t|$ take on values of two meters for 2m-distances ($200 \leq \Delta L_{2m} \leq 500$) much smaller than those corresponding to the $D = 0$ point of Fig. 2. Why does this happen? Further research about this question is in progress.

From all the D values calculated inside the E-sphere, it follows that the determinant D does not vanish along any direction for users with $L < 2.32 \times 10^4 \text{ km}$. For a given direction, the determinant D may vanish once or several times at isolated positions with $L \geq 2.32 \times 10^4 \text{ km}$. Only along scarce directions, quantity D vanishes more than once. There are also many directions without $D = 0$ points. Other 4-tuples and hypersurfaces of constant time, different from those analyzed here (see Sect. 4.1), lead to very similar conclusions.

4.3. *S-errors on spherical surfaces concentric with Earth*

From top to bottom, Fig. 4 shows the values of Δ_R (left panels) and Δ_t (right panels) on spherical surfaces concentric with Earth, whose radius –in kilometers– are $6378 = R_\oplus$ (top) and 1.5×10^4 (bottom). The two surfaces

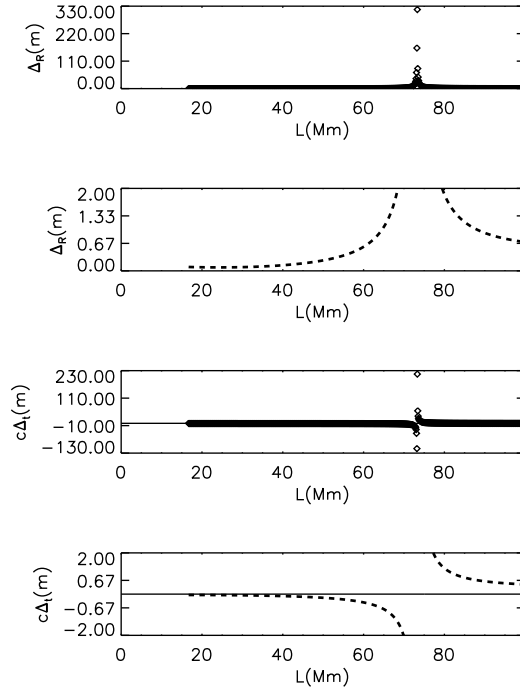


Figure 2: In the top and middle-bottom panels, the same representation as in Fig. 1 is shown. Along the chosen direction quantity D vanishes once. The peak and the discontinuity are associated to the $D = 0$ point. Once the Δ_R and $c|\Delta_t|$ values greater than two meters have been eliminated, the same representation as in Fig. 1 is repeated in the middle-top and bottom panels. All the Δ_R and $c|\Delta_t|$ values smaller than two meters become so visible

are inside the E-sphere and located in the region where the determinant D does not vanish; hence, large values of Δ_R and Δ_t are not expected. Actually, all the values displayed in Fig. 4 range from 0.39 cm to 13 cm . In each of the four panels, grey pixels correspond to the invisibility points on the concentric spheres.

4.4. S -errors versus U -errors

The study of this section is based on Fig. 5. In the top panels of this Figure, all the grey pixels belong to invisibility regions, whereas in the bottom panels, the four big grey spots are the invisibility regions and the remaining grey pixels correspond to Δ_R values greater than two meters.

Since we have calculated U-errors [see Puchades and Sáez (2014)] and

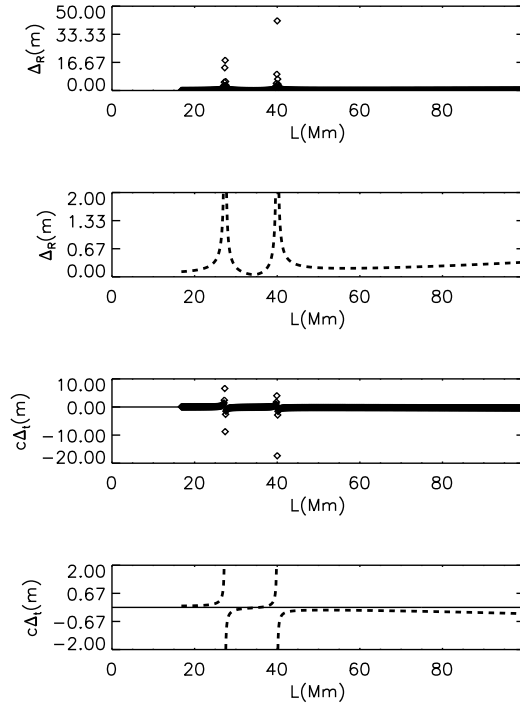


Figure 3: Same representation as in Fig. 2 for a typical direction where D vanishes twice

S-errors at the same places inside the E-sphere, the ratio $\xi = \Delta_{RS}/\Delta_{RU}$ between the Δ_R estimators corresponding to the S-errors (Δ_{RS}) and the U-errors (Δ_{RU}) may be calculated at every visibility point. In Fig. 5, the ξ ratios on four spheres –concentric with Earth– are represented. In the spheres whose radii are $5 \times 10^4 \text{ km}$ (panel 5.c) and $9 \times 10^4 \text{ km}$ (panel 5.d), the ratio ξ has only been calculated at the points where Δ_{RS} is smaller than two meters. So, positions too close to $D = 0$ points are not considered. In panel 5.a, one easily sees that the ξ values are very small on a spherical surface with the Earth’s radius, where the inequality $2.3 \times 10^{-4} < \xi < 8.4 \times 10^{-4}$ is satisfied; hence, the S-errors are negligible against the U-errors on this surface. On the spheres with radii of $1.5 \times 10^4 \text{ km}$ (panel 5.b), $5 \times 10^4 \text{ km}$, and $9 \times 10^4 \text{ km}$, the maximum ξ values are 1.9×10^{-2} , 4.4×10^{-2} , and 3.8×10^{-2} , respectively; hence, in these three cases the maximum values of ξ are of the order of 10^{-2} . It is also observed (panels 5.b to 5.d) that the greatest ξ values (see the color bars) correspond to pixels which are close to grey zones. According to the

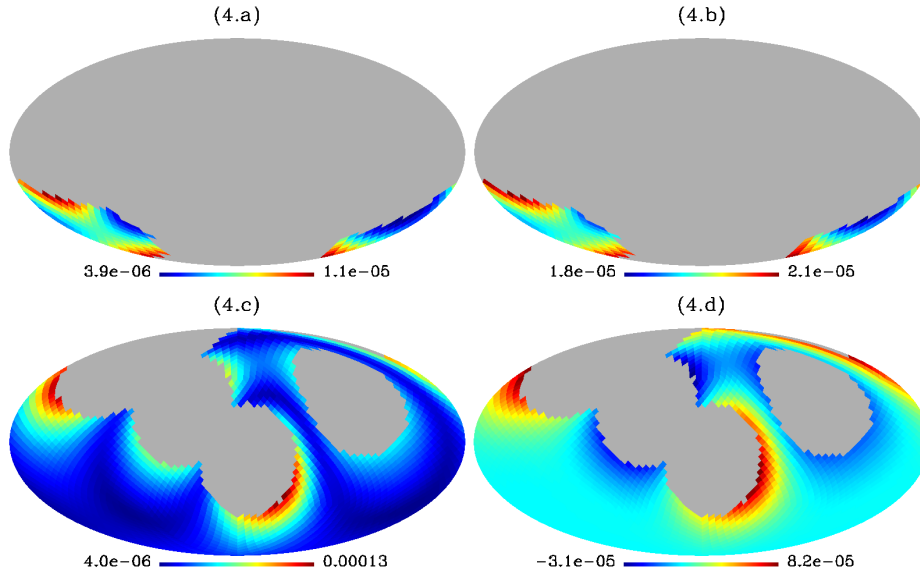


Figure 4: HEALPIX-mollweide maps of the Δ_R (left) and Δ_t (right) estimators (in kilometers) on spherical surfaces with different radii. In the top (bottom) panels, the radius of the surface –in kilometers– is $6378 = R_\oplus$ (1.5×10^4). These surfaces are located in the region, around point E , where the determinant D does not vanish

above description of these zones, this means that the pixels having the largest ξ values are either close to $D = 0$ points or close to invisibility regions.

5. Conclusions and discussion

In Sect. 1, we have outlined a plan for theoretical developments and practical implementations in the field of RPS. We have described the theoretical foundations [points (i) to (v)], two particular but very important RPS approaches [0 and 1 order RPS] and, finally, a novel and well structured program to estimate positioning errors in the framework of RPS [points (1) to (7)]. The total positioning error is the addition of two contributions: the U-error (satellite world lines) and the S-error (photon world lines).

It is believed that, at distances –from Earth– greater than $d_{max} \sim 2 \times 10^4$ km, positioning errors are too big and, consequently, spacecraft navigation based on GNSS is not feasible (see Deng et al. (2013) and references cited therein). In the context of RPS, this is easily understood taking into

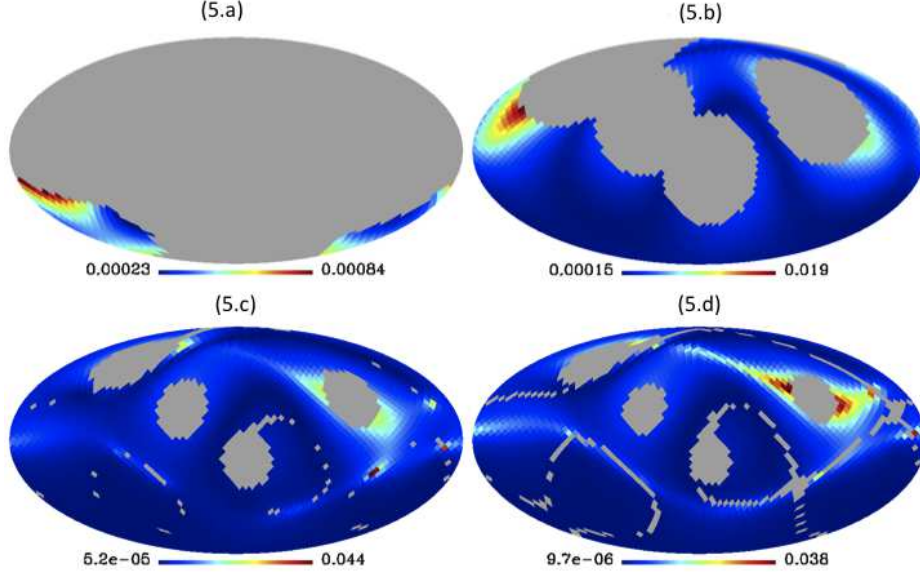


Figure 5: HEALPIX-mollweide maps. The ratio $\xi = \Delta_{RS}/\Delta_{RU}$, between the Δ_R estimators of the S-errors and the U-errors is represented. This ratio is calculated on four spherical surfaces, concentric with Earth, having radii [in kilometers] of $6378 = R_{\oplus}$ [panel a], 1.5×10^4 [panel b], 5×10^4 [panel c], and 9×10^4 [panel d]

account that all the $D = 0$ points are located at distances greater than d_{max} (see Sect. 4.2). Since the S-errors diverge (are large) at (close to) the $D = 0$ points, it seems that spacecraft navigation is only possible for altitudes smaller than $\sim 2 \times 10^4$ km, whereas spacecrafts with altitudes greater than d_{max} may approach $D = 0$ points where positioning errors are too large. Our analysis also suggests the solution to this problem; in fact, in a certain position, a spacecraft may be close to a $D = 0$ point (large positioning errors) for a certain satellite 4-tuple, but the same position may be far from any point of this type for other 4-tuples. This strongly suggests that the spacecraft position may be found anywhere inside the E-sphere by choosing the best 4-tuple at any moment; thus, the proximity to zero points of D might be avoided along the complete world line; which is necessary to make autonomous spacecraft navigation based on GNSS feasible (see also comments

in Sect. 3).

In Sect. 4, the S-error distribution has been studied to conclude that: (A) in the region surrounding Earth where there are no $D = 0$ points, quantities Δ_R and $|\Delta_t|$ take on values smaller than a few tens of centimeters, (B) the S-errors are large where it was expected from the beginning (see the last paragraph of Sect. 3), and (C) positioning quality decays as the distance to the Earth's center increases.

Surrounding every $D = 0$ point, there is a region where the S-errors are larger than 2 m. The size of these regions ranges from hundreds to thousands of kilometers (see Figs. 2 and 3).

The S-errors have been compared with the U-errors for all the users located on four extended spheres. The U-errors have been estimated as in Puchades and Sáez (2014), where an amplitude of 10 m was assumed to simulate the deviations between the nominal and real satellite world lines. Under this assumption, it has been verified that, for the users with S-errors smaller than two meters, the ratio ξ defined in Sect. 4.4 is smaller than ~ 0.05 and, moreover, values of the order 10^{-2} only appear in a few pixels. This means that the S-errors –below a level of two meters– are smaller than five per cent of the U-errors. In this situation, the approach based on the assumption that photons follow null geodesics of M-ST may be applied, at least, for positioning inside the E-sphere with standard accuracy requirements; however, if the amplitude of the satellite deviations becomes –in future– much smaller than ten meters, the U-errors (proportional to this amplitude) will be much smaller and, consequently, the S-errors will not be negligible. In such a case, it must be assumed that photons move in S-ST. The same occurs if we need a high accuracy positioning to deal with some scientific problem.

In standard positioning (not RPS), relativistic corrections are usually applied to satellite motions in GNSS (clock behavior and so on), nevertheless, it is often considered that photons move in Minkowski space-time and, consequently, the S-errors produced by the lensing effect –due to the Earth's gravitational field– are neglected. Here, a certain method has been used –for the first time– to build up robust maps of these positioning errors. These maps of S-errors will be a practical tool since they may be used, from now onwards, to decide if relativistic corrections –due to lensing– are necessary to study a given problem related with positioning on Earth (e.g., carrier signal positioning) or far from Earth (e.g., autonomous spacecraft navigation). For the sake of brevity, only a few maps have been presented in Figs. 4 and 5.

The 1-order RPS may be improved by assuming a slowly rotating Earth

having a realistic mass distribution with small multipoles, which evolves under the action of astronomical objects such as, e.g., the Sun and the Moon, which slightly contribute to the local gravitational field in the positioning region. Fortunately, there are known metrics to properly take into account these improvements (Kerr, Parametrized Post-Newtonian expansions and so on). A metric of the form $\tilde{g}_{\alpha\beta} = \eta_{\alpha\beta} + s_{\alpha\beta} + \zeta_{\alpha\beta}$ seems to be suitable to improve on the 1-order RPS. All the $\zeta_{\alpha\beta}$ quantities will be very small compared with the terms $s_{\alpha\beta}$ (order GM_{\oplus}/R). Since these quantities describe Schwarzschild perturbations, they are neglected in the 1-order RPS.

Nominal satellite world lines corresponding to the metric $\tilde{g}_{\alpha\beta}$ may improve the treatment of U-errors; however, the term $\zeta_{\alpha\beta}$ is not expected to be significant to describe photon motions; in fact, since we have proved that the gravitational influence of the total Earth's mass on the photon world lines is small (Schwarzschild against Minkowski), much smaller gravitational fields—in the positioning zone—such as those due to Earth's multipoles, the Sun, the Moon, and so on, must produce smaller effects on the photons (negligible in practice). The same occurs with the effects of Earth's rotation—which is slow—on the photon world lines, which are expected to be negligible

A first generalization of the 1-order RPS approach could be obtained by including the solar mass; so, the gravitational field would be governed by two sources: a spherically symmetric Earth and the Sun, which could be considered as a point-like mass. In this situation, a system of reference with origin in the Earth-Sun center of mass would be theoretically (physically) inertial (quasi-inertial). The gravitation acceleration produced by the Sun around Earth is $g_{\odot} \simeq 6 \times 10^{-4}g \simeq 1.4 \times 10^{-2}g_{sat}$, where g and g_{sat} are the gravitation accelerations produced by Earth on its surface and on the sphere where the Galileo satellites move, respectively. These numbers show that the solar gravitational field is much smaller than that of the Earth in the positioning region and, consequently, the influence of this field on photon propagation is expected to be negligible. Its effect on the motion of the Galileo satellites is being estimated by us, with the approach suggested at the top of this paragraph.

The study of an RPS improving on the 1-order RPS is beyond the scope of this paper, but our results are important to aid the pursuit of this task in the future. Much research will be necessary before designing and implementing good competitive RPS including error estimations.

We can finally estimate the saving in computer time due to the use of 0-order RPS calculations (instead of 1-order RPS estimates). We have ob-

tained the CPU times taken by our codes to calculate the inertial coordinates x^α (outputs) from the emission coordinates τ^A (inputs). Two codes based on the 0-order and 1-order RPS have been considered. They are multiple precision sequential codes and, consequently, calculations are performed with one thread. The processor is an Intel(R) Xeon(R) CPU E7-4820 (64 bits) at 2 GHz. By working with 32-40 digits the resulting times are $\sim 1 - 2$ ms for the 0-order RPS, and ~ 20 ms for the 1-order RPS; hence, the use of the 0-order RPS –with the exact solution of Coll et al. (2010)– leads to a significant saving of computer time; nevertheless, the 1-order RPS may be also used; in particular, for parallel optimized codes running in modern computers. The same would occur for higher order RPS based on the same methods, but involving more general metrics, nominal satellite world lines, and transfer time functions. All this strongly suggests that, from the point of view of CPU cost, accurate RPS are as feasible as the standard methods used by current GNSS, which are based on relativistic corrections. Researches on RPS are motivated by other positioning aspects detailed above such as, e.g., systematic error estimates, applications to spacecraft navigation, and so on.

ACKNOWLEDGMENTS: This research has been supported by the Spanish Ministry of *Economía y Competitividad*, MICINN-FEDER project FIS2012-33582. We thank B. Coll, J.J. Ferrando, and J.A. Morales-Lladosa for valuable comments.

References

- Abel, J.S., Chaffee, J.W. Existence and uniqueness of gps solutions. IEEE Trans. Aerosp. Electron. Syst., 27, 952-956, 1991.
- Ashby, N. Relativity in the Global Positioning System. Living Rev. Relativ., 6, (1), 2003.
- Bennett, C.L., Larson, D., Weiland, J.L., et al. Nine-year Wilkinson Microwave Anisotropy Probe (WMAP) Observations: Final Maps and Results. Astrophys. J. Supplement, 208, 1 (54pp), 2013.
- Bahder, T.B. Navigation in curved space-time. Am. J. Phys. 69, 315-321, 2001.

- Bini, D., Gerialico, A., Ruggiero, M., et al. Emission versus Fermi coordinates: applications to relativistic positioning systems. *Class. Quantum Grav.* 25, 205011 (11pp), 2008.
- Čadež, A., Kostić, U. Optics in the Schwarzschild spacetime. *Phys. Rev. D*, 72, 104024 (10pp), 2005.
- Čadež, A., Kostić, U., Delva, P. Mapping the space-time metric with a global navigation satellite system, final Ariadna report 09/1301, Advanced Concepts Team, European Space Agency: 1-61, 2010
- Chaffee, J.W., Abel, J.S. On the exact solutions of the pseudorange equations. *IEEE Trans. Aerosp. Electron. Syst.*, 30, 1021-1030, 1994.
- Coll, B., Ferrando, J.J., Morales-Lladosa, J.A. Positioning systems in Minkowski space-time: Bifurcation problem and observational data. *Phys. Rev. D*, 86, 084036 (10pp), 2012.
- Coll, B., Ferrando, J.J., Morales-Lladosa, J.A. Positioning systems in Minkowski space-time: from emission to inertial coordinates. *Class. Quantum Grav.*, 27, 065013 (17pp), 2010.
- Coll, B., Ferrando, J.J., Morales-Lladosa, J.A. From emission to inertial coordinates: an analytical approach. *J. Phys.: Conf. Ser.*, 314, 0121106 (4pp), 2011.
- Delva, P., Kostić, U., Čadež, A. Numerical modeling of a global navigation satellite system in a general relativistic framework. *Adv. Space Res.*, 47, 370-379, 2011.
- Deng, X.P. et al., Interplanetary spacecraft navigation using pulsars. *Adv. Space Res.*, 52, 1602-1621, 2013.
- Górski, K.M., Hivon, E., Wandelt, B.D. Analysis issues for large CMB data sets. In Banday, A.J., Sheth R.K. & Da Costa L. (Eds.), *Proceedings of the MPA/ESO Conference on Evolution of Large Scale Structure*, pp. 37-42, Printpartners Ipskamp Enschede. 1999. arXiv:astro-ph/9812350
- Grafarend, E.W., Shan, J. A closed-form solution of the nonlinear pseudo-ranging equations (GPS). *Artificial satellites, Planetary geodesy* No 28 Special Issue on the XXX-th Anniversary of the Department of Planetary

- Geodesy, Polish Academy of Sciences, Space Research Centre, Warszawa, 31, 133-147, 1996.
- Langley, R.B. Dilution of precision. *GPS World*, 10, 52-59, 1999.
- Misner, C.W., Thorne, K.S., Wheeler, J.A., *Gravitation*. W.H., Freeman and Company, NY. 1973
- Pascual-Sánchez, J.F. Introducing relativity in global navigation satellite systems. *Ann. Phys.*, 16, 258-273, 2007
- Press, W.H., Teukolski, S.A., Vetterling, W.T., Flannery, B.P. *Numerical recipes in fortran 77: the art of scientific computing*. Cambridge University Press, New York, pp. 355-362, 1999.
- Puchades, N., Sáez, D. From emission to inertial coordinates: a numerical approach. *J. Phys.: Conf. Ser.*, 314, 012107 (4pp), 2011.
- Puchades, N., Sáez, D. Relativistic positioning: four-dimensional numerical approach in Minkowski space-time. *Astrophys. Space Sci.*, 341, 631-643, 2012.
- Puchades, N., Sáez, D. Relativistic positioning: errors due to uncertainties in the satellite world lines. *Astrophys. Space Sci.*, 352, 307-320, 2014.
- Sáez, D., Puchades, N. Relativistic positioning systems: Numerical simulations. *Acta Futura*, 7, 103-110, 2013.
- Sáez, D., Puchades, N. Locating objects away from Earth surface: Positioning accuracy. *Springer Proceedings in Mathematics & Statistics*, 80, 391-395, 2014.
- San Miguel, A. Numerical determination of time transfer in general relativity. *Gen. Relativ. Gravit.*, 39, 2025-2037, 2007.
- Schmidt, R.O. A new approach to geometry of range difference location. *IEEE Trans. Aerosp. Electron. Syst.*, 8, 821-835, 1972.
- Synge, J.L. A characteristic function in Riemannian space and its application to the solution of geodesic triangles. *Proc. London Math. Soc.*, 32, 241-258, 1931.

Teyssandier, P., Le Poncin-Lafitte, C. General post-Minkowskian expansion of time transfer functions. *Class. Quantum Grav.*, 25, 145020 (12pp), 2008.